

1 **THERMOPHYSICAL ASPECTS FOR SUSTAINABLE NON-AQUEOUS AMINE SOLVENTS**  
2 **CONTAINING IONIC LIQUIDS IN CO<sub>2</sub> CAPTURE PROCESS**

3 Kalpana Ganesan<sup>1</sup>, Dhanalakshmi Jayaraman<sup>1\*</sup>

4 <sup>1</sup>Solvent Development for Clean Technology Lab, Department of Chemical Engineering,

5 Sri Sivasubramaniya Nadar College of Engineering, Chennai, Tamil Nadu, India

6 Corresponding Author - [\\*dhanalakshmi83@gmail.com](mailto:*dhanalakshmi83@gmail.com)

7  
8  
9  
10  
11  
12  
13  
14  
15  
16  
17  
18  
19

ACCEPTED MANUSCRIPT

20 **Abstract**

21 Climate change is a prime threat to human health and the environment. Carbon dioxide (CO<sub>2</sub>) emissions  
22 play a pivotal role in global warming, the greenhouse gas effect, destroys the ecosystem. This impact of  
23 climate change can be prevented with the help of a solvent-based CO<sub>2</sub> absorption process. In this study,  
24 amine-ionic Liquids (IL) were used as a solvent blend for the CO<sub>2</sub> absorption process. The non-aqueous  
25 solvent blend Monoethanolamine (MEA) - Ionic Liquid (IL) namely tetrabutylammonium  
26 hexafluorophosphate [TBA][PF<sub>6</sub>] and their total concentration was kept at 30 wt% throughout the study.  
27 The thermophysical properties such as density, dynamic viscosity, surface tension, pH and carbon  
28 loading of virgin and carbon-loaded non-aqueous amine-IL have been measured before and after the  
29 absorption process experimentally. This study was extensively carried out for varying temperatures  
30 (293.15 to 333.2 K) and IL concentration (1-2 wt%) at intervals of 10 K and 0.5 wt% respectively. All  
31 the measured thermophysical properties of amine-IL show a significant increase in the IL concentration.  
32 Conversely, it declines while increasing temperature. Higher carbon loading was observed for 2wt%  
33 IL+28wt% MEA, compared to 30wt% MEA, even though increased viscosity was obtained at this  
34 composition. This non-aqueous amine-IL solvent might favor sustainable development in CO<sub>2</sub> capture  
35 process.

36 **Keywords:** Climate change, CO<sub>2</sub> absorption, Carbon loading, amines, Ionic Liquids,

37

38

39

40

41

## 42 1. INTRODUCTION

43 The most common greenhouse gas, carbon dioxide (CO<sub>2</sub>), is considered the primary reason  
44 behind environmental impacts like climate change and global warming. CO<sub>2</sub> is released into the  
45 atmosphere through a variety of industrial processes, including the creation of hydrogen, coal-fired power  
46 stations, oil refineries, and the sweetening of natural gas. The CO<sub>2</sub> is continuously released into the  
47 atmosphere without any restrictions which causes global warming, melting of glaciers and polar ice caps,  
48 a rise in sea level, and extreme weather patterns. The release of CO<sub>2</sub> from various sources accounts for  
49 more than 60% of greenhouse gas; CO<sub>2</sub> is the primary gas responsible for the rise in world temperatures  
50 (Aghel et al. 2022). Several industrial procedures have been developed for extracting CO<sub>2</sub> from gas  
51 stream mixtures such as flue gas and off gas, that include technologies such as physical and chemical  
52 solvent absorption, molecular sieves, carbamation, membrane separation, and cryogenic distillation.  
53 Absorption by physical and chemical solvents is a more advanced method of capturing CO<sub>2</sub> (Amirkhani  
54 et al. 2023). Aqueous alkanolamines and mixes are a popular absorption method that requires amine  
55 scrubbing. Alkanolamines are widely used in most processes due to their high CO<sub>2</sub> reactivity, low cost,  
56 and low hydrocarbon absorption. Alkanolamines, including monoethanolamine (MEA), diethylamine  
57 (DEA), N-methyl-4-piperidinol (MPDL), 2-amino-2-methyl-1-propanol (AMP), and N-  
58 methyldiethanolamine (MDEA), are widely used chemical absorbents in industry. MEA is the  
59 benchmark solvent for CO<sub>2</sub> absorption in fossil-fueled thermal industries (Kontos et al. 2023).  
60 Alkanolamines do, however, have a variety of disadvantages, like high volatility, thermal and oxidative  
61 degradation, equipment corrosion, high operating costs, higher energy consumption, and harmful  
62 environmental pollution (Elmobarak et al. 2023). To overcome these drawbacks for CO<sub>2</sub> capture, looking  
63 into better alternative technologies was required. Ionic liquids are a recently discovered category of  
64 potential solvents. Compared to frequently used aqueous amines, they can provide various advantages.

65 Ionic liquids, or molten salts, arise when an asymmetric organic cation and an inorganic or  
66 organic anion mix. The appealing properties of ILs include their low melting point, non-volatility, strong  
67 thermal and chemical stability, and low vapor pressure. Because of these qualities, ILs are called "green  
68 solvents" or "environment-friendly solvents." Numerous researchers have reported favorably on using  
69 ILs in numerous industrial and academic sectors. Catalytic processing, enzymatic processes,  
70 electrochemical usage, acid gas treatment, processing of polymer, and battery electrolyte are just a few  
71 of the IL applications. A few ammonium-based ILs, as well as several IL classes such as pyridinium,  
72 phosphonium, pyrrolidinium, and imidazolium, have previously been identified (Shojaeian et al. 2021).  
73 Room-temperature ionic liquids (RTILs) absorb CO<sub>2</sub> by physical absorption and have a limited capacity  
74 and selectivity. Task-specific ionic liquids (TSILs) are designed by changing the cation or anion and  
75 lengthening the chain to improve selectivity, solubility for certain gases, or catalytic activity. Anions  
76 have a greater influence on the solubility of ILs in CO<sub>2</sub> absorption than cations (Yan et al. 2024). Anions  
77 that have recently been described in the literature include hexafluorophosphate [PF<sub>6</sub>], tetrafluoroborate  
78 [BF<sub>4</sub>], and bis(trifluoromethylsulfonyl)imide [Tf<sub>2</sub>N]. [Tf<sub>2</sub>N]-based ILs have considerable CO<sub>2</sub> solubility.  
79 The [Tf<sub>2</sub>N] anion's extraordinary CO<sub>2</sub> solubility might be attributable to its enormous size (Orhan, 2021).  
80 Ionic liquids functionalised with amines, known as amino acid-based ionic liquids (AAILs), were created  
81 to increase ILs' ability to absorb CO<sub>2</sub>. AAILs are more capable of absorbing CO<sub>2</sub> than most pure amino  
82 acids, ethanolamine derivatives, and amino acid salts. According to Noorani et al. (2021), these ILs boost  
83 the capacity of CO<sub>2</sub> absorption by chemisorption.

84 Perumal et al. (2020) studied the physical characteristics by varying the temperature (293.4 to  
85 333.4 K) and IL content (10 to 50 wt%) of ammonium functionalised ionic liquids at intervals of 10 wt%  
86 and 10 K. The study found that the concentration, density, and surface tension of tetrabutylammonium  
87 bromide [TBA][Br] increased, but tetrabutylammonium acetate [TBA][OAc] and tetrabutylammonium  
88 hydroxide [TBA][OH] showed the reverse tendency. The result shows that [TBA][Br] and water have a

89 stronger molecular bond than other ILs. All aqueous ILs have an increase in dynamic viscosity with IL  
90 concentration. It is well known that ILs' physical properties deteriorate with temperature. The  
91 thermophysical properties of three binary liquid solutions of the MDEA, DEA, and AMP with the ionic  
92 liquid 1-ethyl-3-methylimidazolium acetate ([Emim][Ac]) T = 293.15–333 at intervals of 10 K was  
93 studied by (Shojaeian et al. 2021). Based on the findings, temperature increases resulted in a drop in  
94 viscosity, density, and refractive index for both pure and binary systems. Because of the mixture's  
95 intricate behaviour, each system's effect of concentration on the thermophysical parameters of the  
96 investigated solutions was distinct, and no overarching pattern was discovered.

97 The impact of density of ammonium-based IL, aqueous tetrapropylammonium hydroxide  
98 (TPAOH) at various temperatures (298.15 to 333.15 K) and concentrations (5, 10, 15, 20, and 25 wt%)  
99 was studied by (Kartikawati et al. 2018). It was shown that density increases along with temperature and  
100 IL concentration. This happens as a result of the molecule's tendency to disperse when both temperature  
101 and kinetic energy increase. Yusoff et al. (2014) studied the surface tension and heat capacity of different  
102 types of ILs, namely 1-butyl-3-methylimidazolium dicyanamide, 1-butyl-3-methylimidazolium  
103 tetrafluoroborate ([bmim][BF<sub>4</sub>]), and [bmim][DCA]. The following trend was observed when  
104 temperature increases and ionic liquid concentration rises the surface tension tends to decrease. The heat  
105 capacity of the mixes increases as temperature rises and ionic-liquid concentration decreases. Aqueous  
106 ionic liquid-amine hybrids may be a superior solvent for CO<sub>2</sub> collection due to their high loading  
107 capacity, higher absorption rate, and energy-efficient method. Only a limited number of published  
108 investigations could be found on the non-aqueous hybrid solvent composed of monoethanolamine  
109 (MEA), tetrabutylammonium hexafluorophosphate [TBA][PF<sub>6</sub>], and ethanol. Physical characteristics of  
110 the solvents are thought to be particularly important when examining the rate of absorption and  
111 absorption capacity. The study of physicochemical features at a lower temperature (293.15K) is required  
112 for CO<sub>2</sub> absorption process. In this work, the physical property behavior of monoethanolamine (MEA),

113 non-aqueous tetrabutylammonium hexafluorophosphate [TBA][PF<sub>6</sub>] and ethanol mix at a range of IL  
114 concentrations (1-2 wt%) and temperatures (293.15-333.4 K) was studied.

## 115 **2. MATERIALS AND METHODS**

116 The current investigation employed a minimum purity of 99 weight percent (Laboratory Grade)  
117 monoethanolamine (MEA). TetraButylAmmonium Hexafluorophosphate ([TBA][PF<sub>6</sub>]), a highly pure  
118 ionic liquid from Spectrochem was utilised. The concentrations of MEA and IL ([TBA][PF<sub>6</sub>]) are only  
119 stated in weight percent. The animated flue gas of 15% CO<sub>2</sub> and 85% nitrogen was commercially  
120 purchased. The physical properties were measured by various instruments and the details were mentioned  
121 in previous work (Perumal et al. 2021).

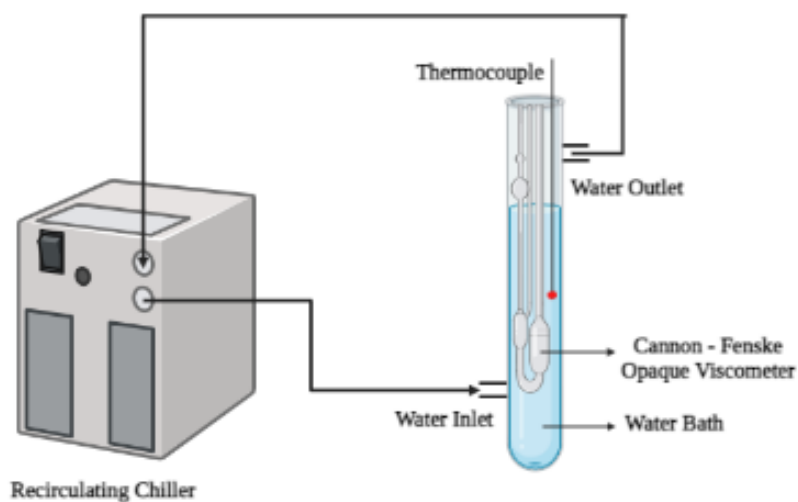
### 122 **2.1 Density Measurement**

123 The density of MEA and non-aqueous [TBA][PF<sub>6</sub>] mix (1 to 2 wt%) was computed by adding  
124 the sample to the specific gravity bottle (5 cm<sup>3</sup>). The bottle was maintained in the water bath with a  
125 temperature control. The density was calculated for a range of temperatures (293.15-333.15 K). The  
126 sample was given 10 to 20 minutes to reach thermal equilibrium at each temperature rise of 10 K (Khan  
127 et al. 2017). Each experiment is calibrated by measuring the density of Ethanol as a reference fluid.

### 128 **2.2 Dynamic Viscosity and Surface Tension Measurement**

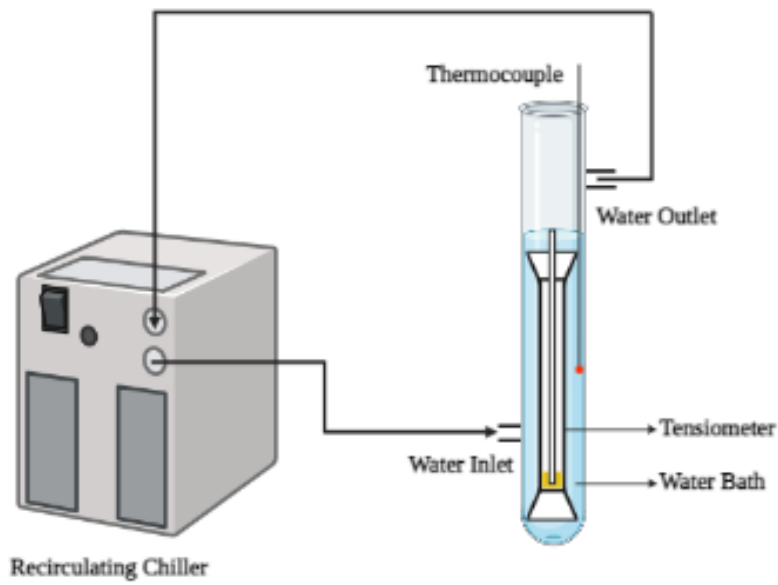
129 The surface tension and dynamic viscosity of blends of non-aqueous [TBA][PF<sub>6</sub>] and MEA was  
130 measured experimentally for concentrations (1 to 2 wt%) and temperatures (293.15 to 333.15 K). **Figure**  
131 **1a** illustrates the cooling setup that included a chiller, a water bath with a temperature controller, a  
132 cylindrical tank with a viscometer, and a similar setup for the tensiometer. The chilled water is  
133 recirculated at the proper temperature from the chiller to the cylindrical vessel. A K-type thermocouple  
134 ( $\pm 0$  K accuracy) was installed inside the cylindrical jar to detect temperature. A similar arrangement is  
135 done with tensiometer for measuring surface tension as shown in **Figure 1b**.

136 The heating setup shown in **Figure 1c** consists of a heating coil, a water bath with a temperature  
137 controller, a cylindrical tank with a viscometer. The heating coil, which is located inside the water  
138 container, is connected to the temperature controller and power supply. The temperature controller keeps  
139 the temperature stable during the operation. Hot water is recirculated at the appropriate temperature from  
140 the heating bath to the cylindrical vessel. A K-type thermocouple ( $\pm 0$  K accuracy) was installed inside  
141 the cylindrical jar to detect temperature. A similar arrangement is done with tensiometer for measuring  
142 surface tension as shown in **Figure 1d**. Each experimental run is calibrated using measurements of  
143 ethanol's surface tension and dynamic viscosity.



144

145 **Figure 1a.** Schematic representation of dynamic viscosity measurement in chiller setup

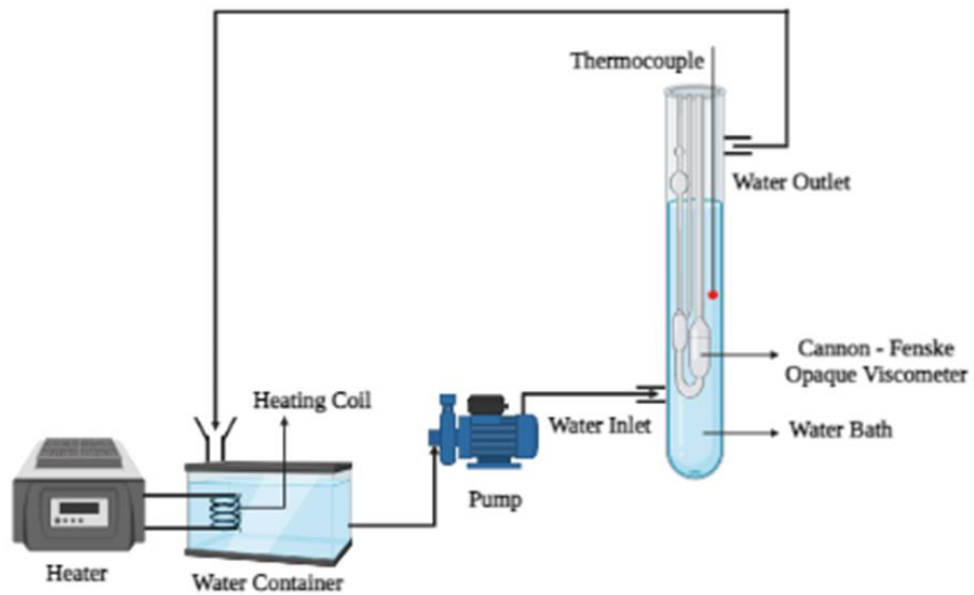


146

147

**Figure 1b.** Schematic representation of surface tension measurement in chiller setup

148



149

150

**Figure 1c.** Schematic representation of dynamic viscosity measurement in heating setup

151



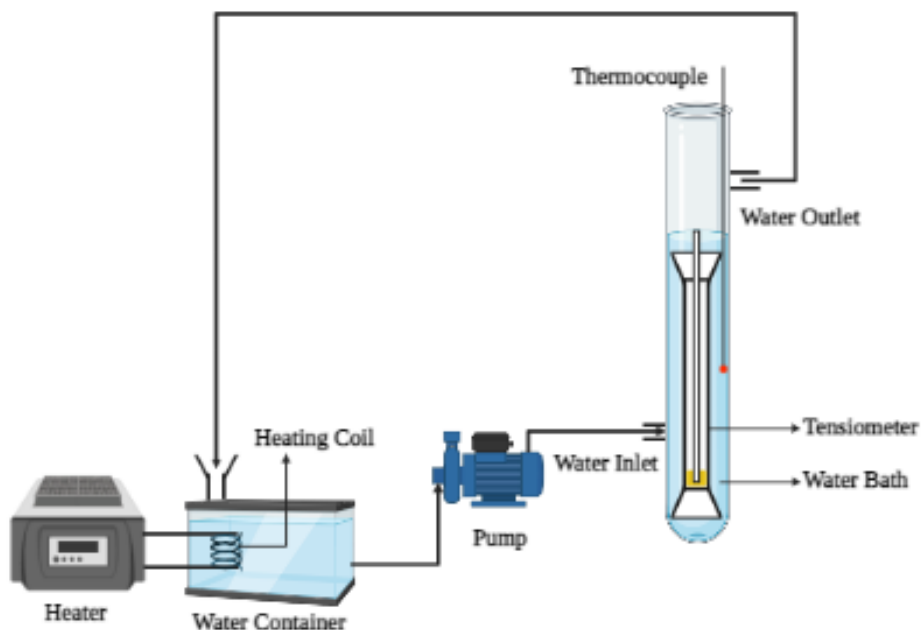


**Figure 1d.** Schematic representation of surface tension measurement in heating setup

### 3. RESULTS AND DISCUSSION

#### 3.1 Density

##### 3.1.1 Impact of Temperature and Concentration on Density

Volume fluctuates with temperature, which causes a change in density. The molecules of the solvent mixture push away as its temperature rises because of the rise in kinetic energy. The result is a decrease in density and an increase in material volume. The similar behaviour is reported by Rahim et al. (2023). The reduced molecular interactions between molecules result in lesser density because the kinetic energy of molecular interaction between the ionic liquid and solvent becomes weak (Wu et al. 2020).

The effect of IL concentration on density was investigated for non-aqueous [TBA][PF<sub>6</sub>] and MEA blends at various concentrations. Density increases as the concentrations of [TBA][PF<sub>6</sub>] in the MEA mix increase. The Coulombic forces in an ionic liquid strongly attract the unlike charges, when [TBA][PF<sub>6</sub>]

166 is added to MEA, the volume of IL's ion pair increases and there is a rise in density. Furthermore,  
167 increasing the concentration of ionic liquids resulted in a rise in the density of the solution at constant  
168 temperature. This is owing to the larger molecular size of fluoride anion, which causes the weaker contact  
169 between cation and anion, resulting in a greater density of ILs that was observed, and similar behaviour  
170 was also described by Perumal et al. (2020).

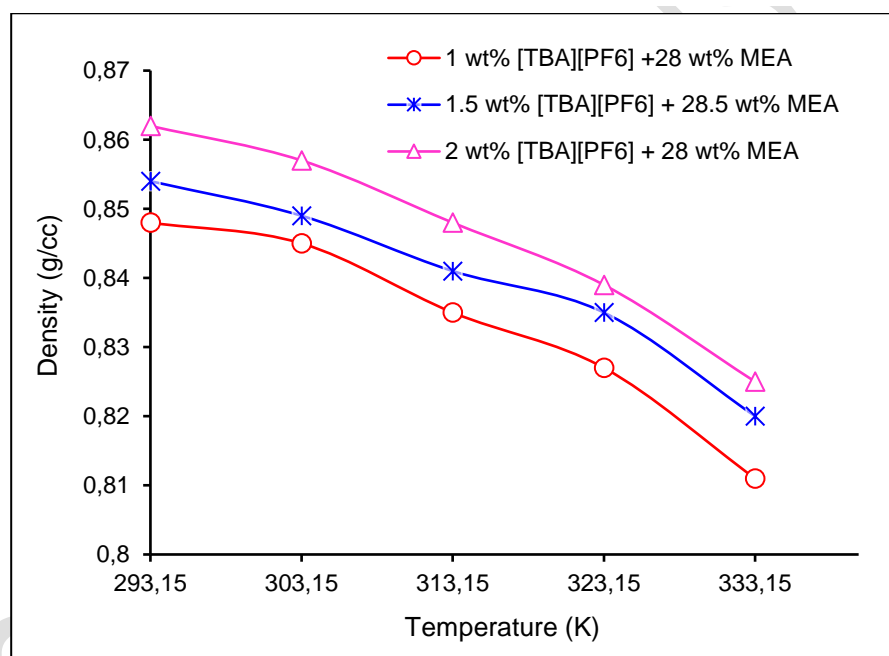
171 It is possible that the molecules exhibit moderate intermolecular interactions at higher temperatures and  
172 significant intermolecular forces at greater concentrations of ionic liquids. (Baj et al. 2013). The average  
173 kinetic energy of molecules in a material increases with temperature. The molecules travel quicker and  
174 collide more frequently, which increases the distance between them. (Mazari et al. 2021). The density of  
175 the substance reduces as the distance between molecules widens. This behavior is noticed as gas density  
176 is directly proportional to pressure and inversely proportional to temperature (Halim et al. 2016). **Figure**  
177 **2a** shows for the specified solvent blend of MEA and [TBA][PF<sub>6</sub>], density decreases with increasing  
178 temperature.

### 179 **3.1.2 Impact of Time and Concentration on Density**

180 The density and molecular volume of the ionic liquids are related to the amount of CO<sub>2</sub> absorption  
181 (Yunus et al. 2019). Density increases as the CO<sub>2</sub> solubility increases which causes the volume change.  
182 As the concentration of IL increases, CO<sub>2</sub> and mixture form new bonds which will result in new  
183 molecules thereby increasing the density of the mixture. The density for different concentration of the  
184 non-aqueous blends of MEA and IL was investigated for different absorption time. In the virgin solution  
185 MEA interacts with [TBA][PF<sub>6</sub>] resulting in huge voids due to steric hindrance from bulk molecules of  
186 [TBA][PF<sub>6</sub>]. As absorption progress with the time, increase in density of the solvent mixture was noted.  
187 This trend was seen due to the chemical reactions and van der Waals attraction property of CO<sub>2</sub> molecules  
188 with solvents free space (Wang et al. 2023). During CO<sub>2</sub> absorption, the CO<sub>2</sub> molecules occupy the free

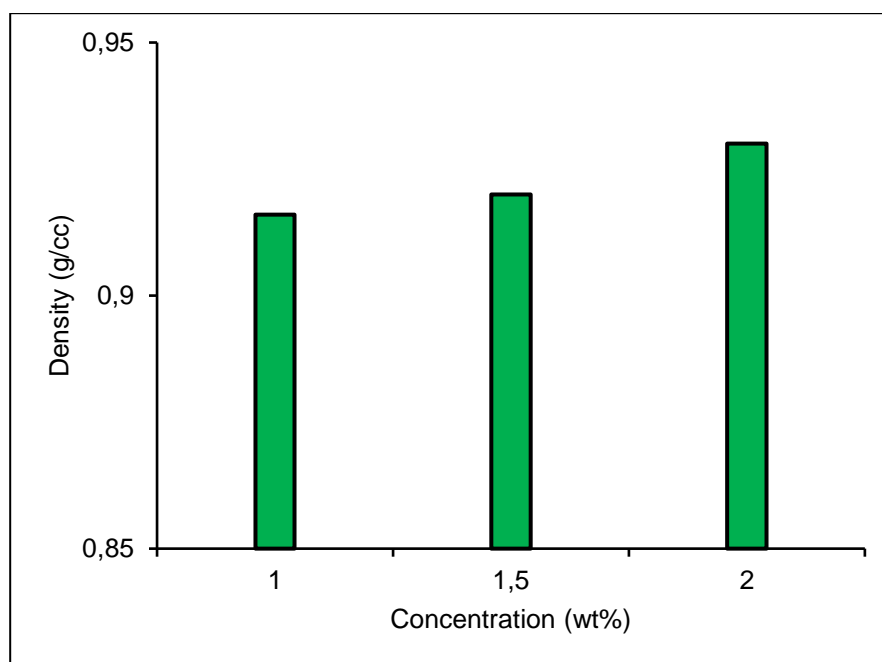
189 spaces accessible on the solvent's surface due to the polarity effect. **Figure 2b** indicates that the density  
190 is linearly proportional to concentration of IL due to the accumulation of more CO<sub>2</sub>. As an amount of  
191 time passes CO<sub>2</sub> absorption rises, causing CO<sub>2</sub> to accumulate in the mixture's void spaces and form new  
192 bonds, increasing density. The experimental findings of density for the carbon loaded solution is shown  
193 in **Figure 2c**. The concentration of the IL is of the order 2 wt% [TBA][PF<sub>6</sub>] > 1.5 wt% [TBA][PF<sub>6</sub>] >  
194 1wt% [TBA][PF<sub>6</sub>]. Density increases due to the increase of molecular weight of the mixture (Ramkumar  
195 et al. 2019).

196



197

198 **Figure 2a.** Temperature and concentration dependence of density of non-aqueous MEA-  
199 [TBA][PF<sub>6</sub>].  
200



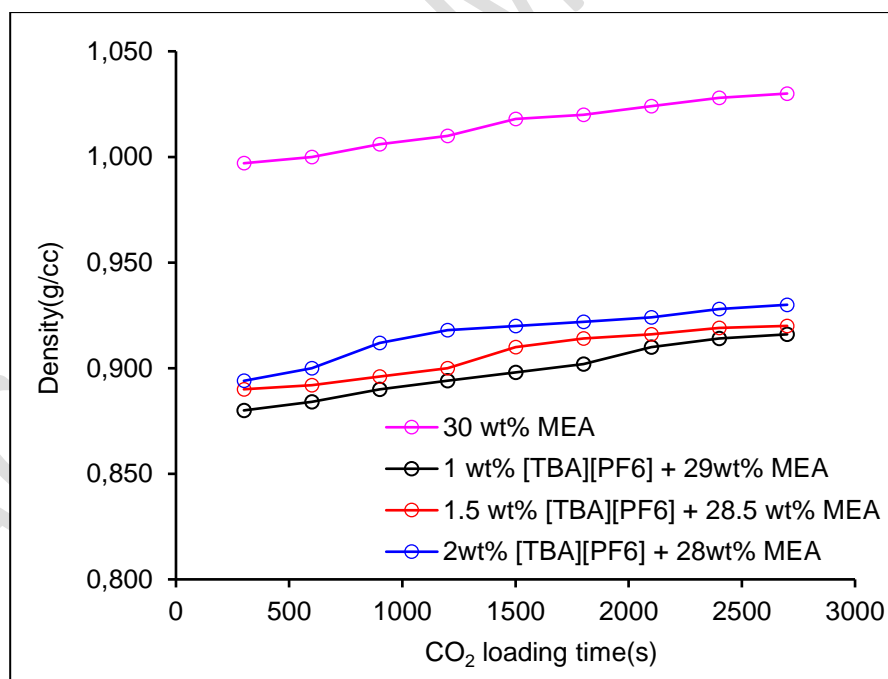
201

202

**Figure 2b.** Concentration dependence of density of non-aqueous MEA-[TBA][PF<sub>6</sub>] after absorption

203

204



205

206

**Figure 2c.** Time and concentration dependence of density of non-aqueous MEA-[TBA][PF<sub>6</sub>] after absorption

207

## 208 3.2 Dynamic Viscosity

### 209 3.2.1 Impact of Temperature and Concentration on Dynamic Viscosity

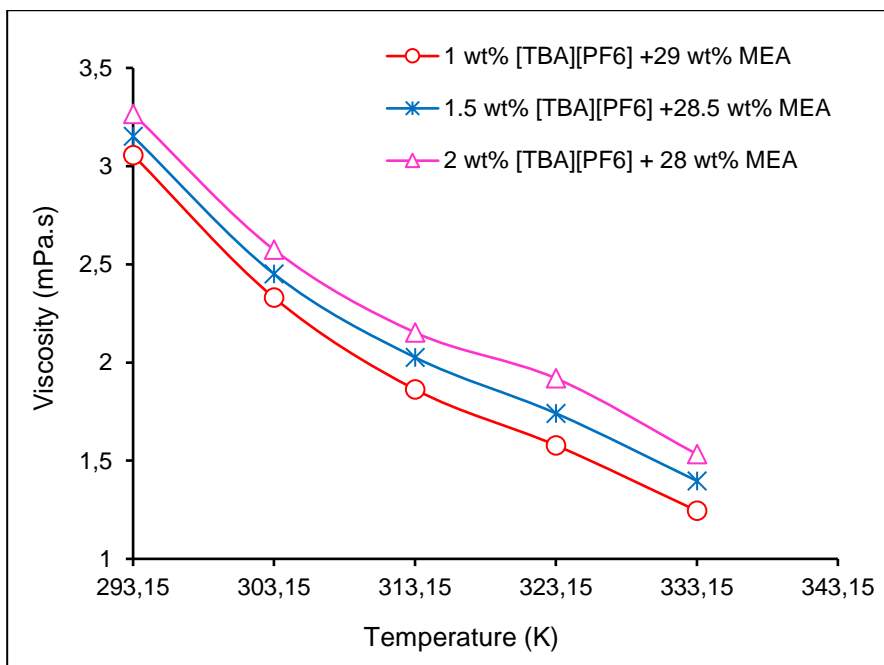
210 Viscosity is the most important physical component of the gas separation process. As a result, the  
211 investigation of temperature and concentration on viscosity is essential to understand gas-liquid kinetics  
212 in solvents for a wide range of industrial applications (Wei et al. 2020). The effect of temperature and  
213 concentration on viscosity of non-aqueous MEA-IL blends is illustrated in **Figure 3**. It has been shown  
214 that dynamic viscosity of the non-aqueous MEA-IL blends decreases considerably as temperature rises  
215 for various concentration ranges (Li et al. 2021). The concentration directly affects the dynamic viscosity  
216 of the non-aqueous ILs examined. It was noticed that the viscosity in MEA-[TBA][PF<sub>6</sub>] mixes increased  
217 with the increase in IL concentration (Hafizi et al. 2021).

218 Viscosity rises as IL concentration in solvent mixtures rises because more molecules become present and  
219 create new interactions with one another. In the study of CO<sub>2</sub> absorption of IL systems, Zhang et al.  
220 (2012) showed that Henry's constant falls as more ILs are included in the system, and it was observed  
221 the primary cause was increased viscosity, which results from the addition of additional ILs. Higher  
222 kinetic forces between molecules cause faster movement, which reduces intermolecular interaction and  
223 resulting in lower viscosity at higher temperatures (Boualem et al. 2022).

224 When the IL concentration rises, the viscosity of the solvent mixture also rises. Viscosity rises as IL  
225 concentration in solvent mixtures rises because this results in more molecules entering the mixture and  
226 forming new interactions with one another (Latini et al. 2022). Opposing charges passing one another  
227 and disrupting the network put limits on ion mobility within an ionic liquid, which increases viscosity as  
228 the concentration rises. The barrier to mobility is decreased by the presence of CO<sub>2</sub> by reducing the  
229 intermolecular contacts between the cations and anions. Due to the strong solubility and phase behavior  
230 of CO<sub>2</sub> in ILs, this has occurred (Theo et al. 2016). It was seen that viscosity increases with the solubility

231 of CO<sub>2</sub>. Carbon-rich solutions exhibit higher viscosity during absorption due to greater hydrogen bonding  
232 between molecules. Higher viscosity hinders mass transfer kinetics between solvent blend and CO<sub>2</sub>,  
233 resulting in lower absorption capacity. The similar behaviour is reported in Perumal et al. (2023).

234



235

236 **Figure 3.** Temperature and concentration dependence of viscosity of non-aqueous  
237 MEA-[TBA][PF6]

237

### 238 3.3 Surface Tension

#### 239 3.3.1 Impact of Temperature and Concentration on Surface Tension

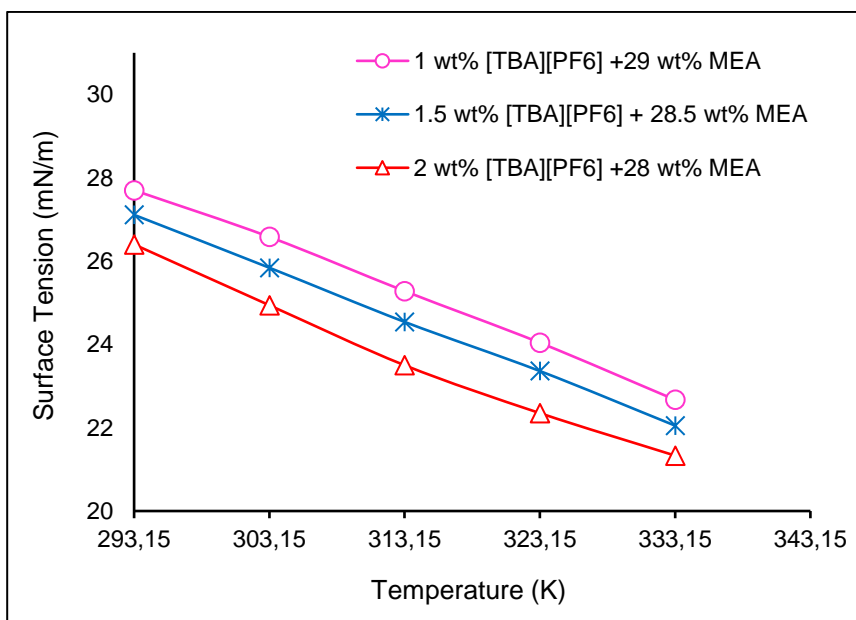
240 Experiments were conducted to study the impact of temperature and concentration on surface tension at  
241 temperatures ranging from 293.15 to 333.15 K. **Figure 4a** shows that the surface tension data decreases  
242 linearly as the concentration of the ionic liquids increases. With an increase in the ionic liquid  
243 concentration, the overall intermolecular tensions between the molecules of the solution decrease,  
244 resulting in a decrease in surface tension (Hasib-ur-Rahman et al. 2010). The MEA-IL [TBA][PF<sub>6</sub>]

245 mixtures surface tension decreased as the temperature was increased for all concentration levels as shown  
246 in **Figure 4a**. At greater temperatures, hydrogen bonding between molecules may weaken, which might  
247 explain the phenomenon. The molecules in the solvent mix have greater kinetic energy due to increased  
248 temperature and move with greater velocity. As a result, the thermal mobility of the molecules increases,  
249 which lessens their intermolecular attraction to one another and causes surface tension to drop at higher  
250 temperatures. Surface tension decreases with increasing [TBA][PF<sub>6</sub>] concentration in MEA mixes  
251 because of fewer molecular interactions, which lowers the gas-liquid interface between the solvent  
252 molecules. The similar behaviour is reported in literature (Amirchand et al. 2022).

### 253 **3.3.2 Impact of Time and Concentration on Surface Tension**

254 Cohesive forces that hold the molecules at a liquid's surface together are measured by surface  
255 tension, when a liquid comes into contact with a gas, such as when carbon dioxide is absorbed into a  
256 liquid, the presence of both the gas and any dissolved molecules, such as ionic liquids, can change the  
257 liquid's surface tension. After carbon loading surface tension increases linearly with concentration due  
258 to high intermolecular forces between ionic liquid solution with CO<sub>2</sub> after absorption as shown in **Figure**  
259 **4b**. Additionally, the ILs may build up at the liquid-gas interface over time and create a stable interfacial  
260 layer there. This layer may serve to raise the liquid's surface tension by effectively separating the liquid  
261 phase from the gas phase and reducing the surface area of the liquid that comes into contact with the gas.  
262 The IL concentration in the liquid may influence the stability and thickness of this interfacial layer, as  
263 well as the liquid's surface tension (Zacchello et al. 2017). Therefore, the increase in surface tension with  
264 time and concentration of IL after carbon dioxide absorption can be attributed to the pH changes, the  
265 intermolecular interactions of the ILs, and liquid-gas interface formation (Torralba-Calleja et al. 2013).  
266 Based on these findings, increasing the concentration of ILs in virgin solution lowered surface tension  
267 due to the likelihood of lower molecular interactions (Perumal et al. 2023). The surface tension increases

268 for the MEA and [TBA][PF<sub>6</sub>] blends as the CO<sub>2</sub> absorption progress. **Figure 4c** illustrates surface tension  
269 increases linearly with time due to the increase in intermolecular forces between CO<sub>2</sub> and mixtures. The  
270 net intermolecular forces of attraction between molecules increase over time during CO<sub>2</sub> absorption in  
271 the mixture resulting in increased surface tension.



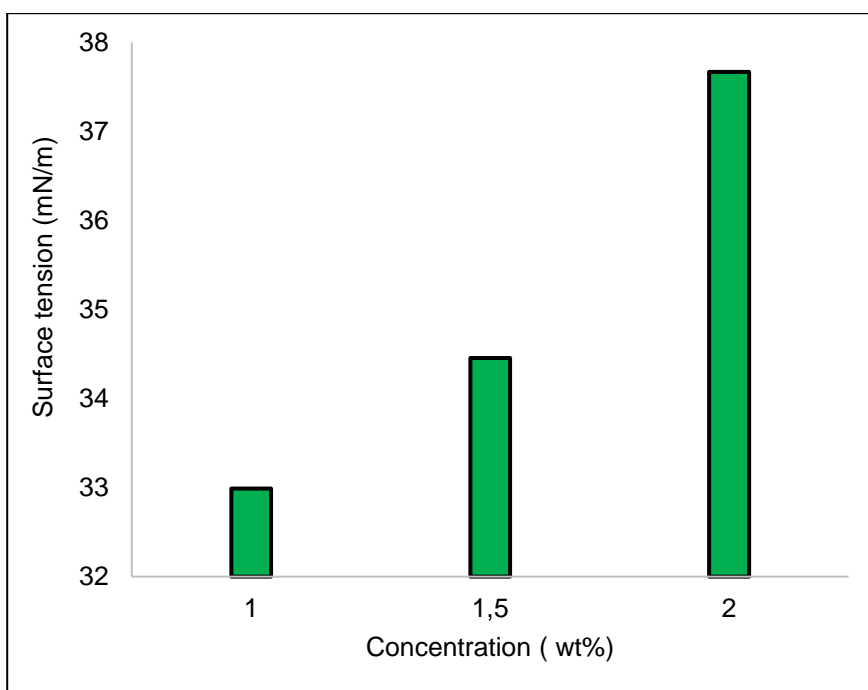
272

273 **Figure 4a.** Temperature and concentration dependence of surface tension of non-aqueous

274

MEA-[TBA][PF<sub>6</sub>]





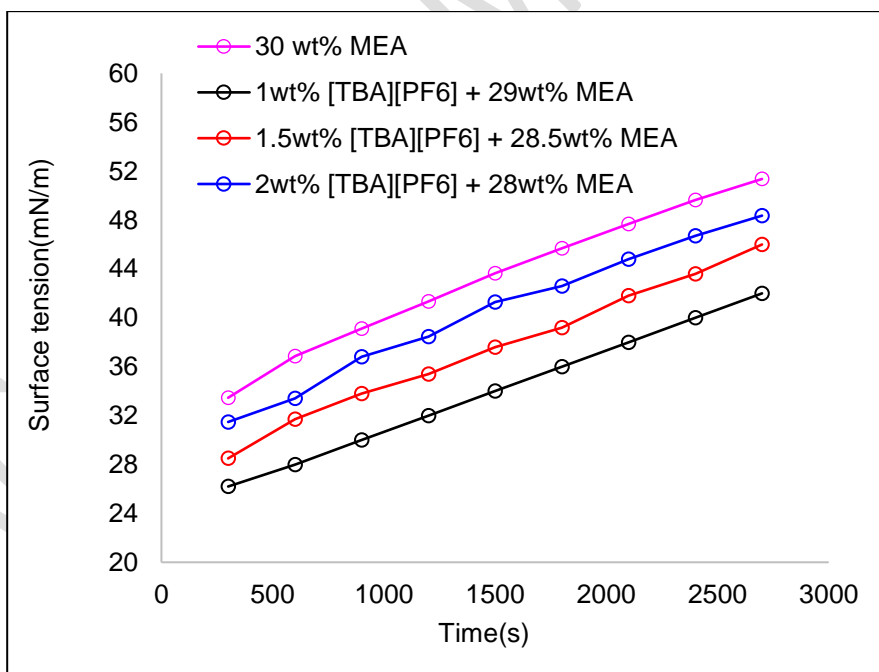
275

276

**Figure 4b.** Concentration dependence of surface tension of non-aqueous MEA-[TBA][PF<sub>6</sub>] after

277

absorption



278

279

**Figure 4c.** Time and concentration dependence of surface tension of non-aqueous MEA-

280

[TBA][PF<sub>6</sub>] after absorption.

## 281 3.4 pH

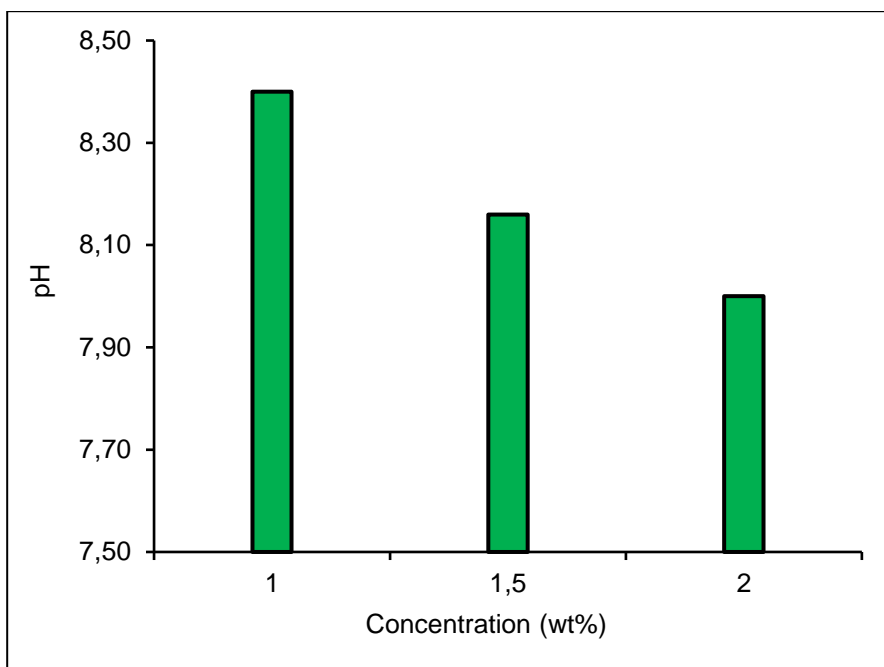
### 282 3.4.1 Impact of Concentration on pH

283 pH is a crucial parameter in selecting suitable solvent for CO<sub>2</sub> absorption. When the concentration  
284 of CO<sub>2</sub> in the solvent mixture increases pH decreases due to the increase in [TBA][PF<sub>6</sub>] which is weakly  
285 basic as compared to MEA. The Debye-Huckel equation states that as an aqueous solution's ionic strength  
286 increases, the activity of the hydroxide ion decreases. By improving the solubility of CO<sub>2</sub> in the solution,  
287 [TBA][PF<sub>6</sub>] can be added to this mixture to further raise the acidity of the solution. It has been  
288 demonstrated that [TBA][PF<sub>6</sub>] has a high CO<sub>2</sub> solubility and can increase the solubility of CO<sub>2</sub> in the  
289 solvent mixture (Numpilai et al. 2024). It was found the interaction of [TBA][PF<sub>6</sub>], MEA, and ethanol  
290 may form several weak acids, increasing hydrogen ions levels while decreasing pH levels in the solution.  
291 Drop in pH for the solvent blends was noted during the absorption due to presence of CO<sub>2</sub> (Choi et al.  
292 2021).

### 293 3.4.2 Impact of Concentration and Time on pH

294 The concentration of hydrogen ions (H<sup>+</sup>) in a solution is represented by its pH value. A weak  
295 acid, such as ethanoic acid or propanoic acid, can nevertheless be formed when carbon dioxide dissolves  
296 in a non-aqueous solvent, such as an organic solvent like ethanol or acetone (Shukla et al. 2019). **Figure**  
297 **5a** shows an increase in the concentration of hydrogen ions (H<sup>+</sup>) in the solution. As a result of the weak  
298 acid being produced from carbon dioxide and the solvent leads to a fall in pH (Kaviani et al. 2018). The  
299 pH lowers over time as a result of the CO<sub>2</sub> gas being absorbed by the combination of ionic liquids as  
300 shown in **Figure 5b**.

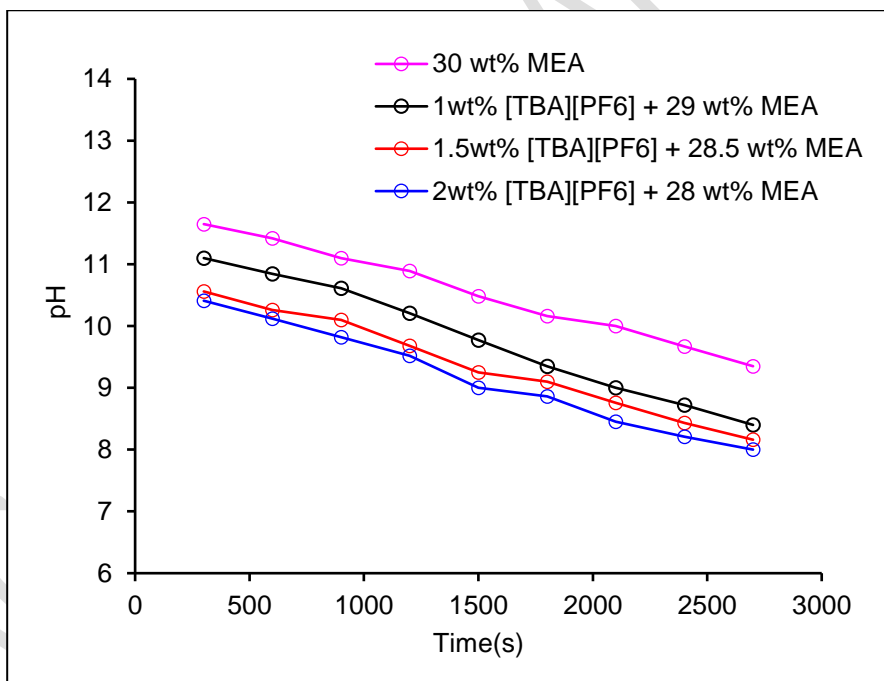
301



302

303

**Figure 5a.** Concentration dependence of pH of non-aqueous MEA-[TBA][PF<sub>6</sub>] after absorption



304

305

**Figure 5b.** Time and concentration dependence of pH of non-aqueous MEA-[TBA][PF<sub>6</sub>]

306

after absorption

307

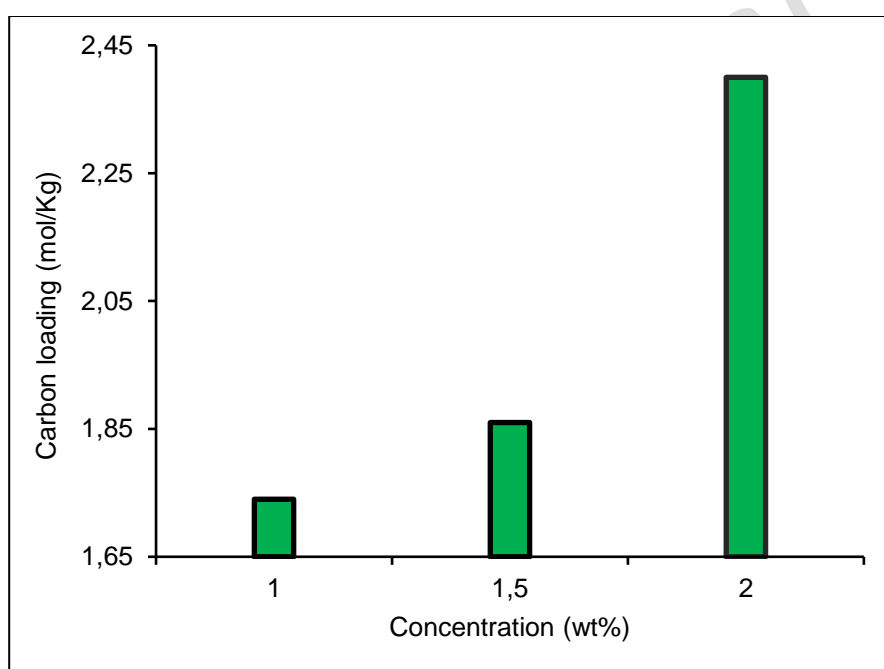
## 308 3.5 Carbon Loading

### 309 3.5.1 Impact of Concentration and Time on Carbon Loading

310 Ma et al. (2018) showed that the formation of a solid network of anions and cations, with CO<sub>2</sub>  
311 filling the interstices in the fluid, is what causes CO<sub>2</sub> solubility in ionic liquids. The slight differences in  
312 cation structure do not, however, have a major impact on the dominant CO<sub>2</sub>-anion interactions. As a  
313 result, in ionic liquids, anion affects CO<sub>2</sub> solubility whereas the cation does not affect the process (Yang  
314 et al. 2024). **Figure 6a** illustrates the effect of carbon loading on solvent mixture concentration.

315 The cation is considered to play a supportive function in the breakdown of CO<sub>2</sub> and anion is  
316 thought to perform a major role. The researchers discovered that CO<sub>2</sub> interacts largely with the [PF<sub>6</sub>]  
317 anion, independent of the cation. Previous studies using in situ ATR-IR spectroscopy shown that the  
318 anion [PF<sub>6</sub>] and CO<sub>2</sub> might interact positively. According to the spectroscopic data, the interaction is  
319 Lewis acid-base in nature, with the anion functioning as the Lewis base and the CO<sub>2</sub> as the Lewis acid.  
320 The spectroscopic results also provide compelling evidence of the interaction between CO<sub>2</sub> and the [PF<sub>6</sub>]  
321 anion. According to Brennecke et al. (2010) the free volume mechanism is predicted to play a significant  
322 role in the dissolution of CO<sub>2</sub> because anion-CO<sub>2</sub> interactions alone are insufficient to explain the  
323 solubility. Given that the liquid volumes of ILs are not significantly altered when large amounts of CO<sub>2</sub>  
324 are dissolved, it is expected that CO<sub>2</sub> molecules will be hosted in the liquid's free spaces (cavities) during  
325 a free-volume process. The more CO<sub>2</sub> can be dissolved by an anion the more fluoro groups it possesses.  
326 This was done by investigating a wide range of ILs, and it was discovered that Henry's constants of CO<sub>2</sub>  
327 may be related to the excess enthalpy of CO<sub>2</sub> dissolution in IL (Abraham et al. 2019). This demonstrated  
328 that increased solubilities are connected with higher combination exothermicities. Moreover, the  
329 anticipated intermolecular interactions (van der Waals, hydrogen bonds, and electrostatic interactions)  
330 between species in a fluid phase. The effects of different interactions on the solubility of CO<sub>2</sub> in Ionic

331 Liquids were studied, and the findings show that van der Waals forces dominate the process (Shohrat et  
332 al. 2022). The influence of absorption time and concentration on carbon loading was studied  
333 experimentally. **Figure 6b** illustrates carbon loading for solvent blends increases with increased CO<sub>2</sub>  
334 absorption time. It was noted that addition of IL to MEA caused increased carbamate production leading  
335 to better CO<sub>2</sub> absorption. It was also noted that the presence of fluorinated anion of the IL promotes CO<sub>2</sub>  
336 loading in biphasic absorbents. This behaviour has already been observed in literature (Yang et al. 2023).  
337



338

339 **Figure 6a.** Concentration dependence of carbon loading of non-aqueous [TBA][PF<sub>6</sub>]-MEA after  
340 Absorption

341

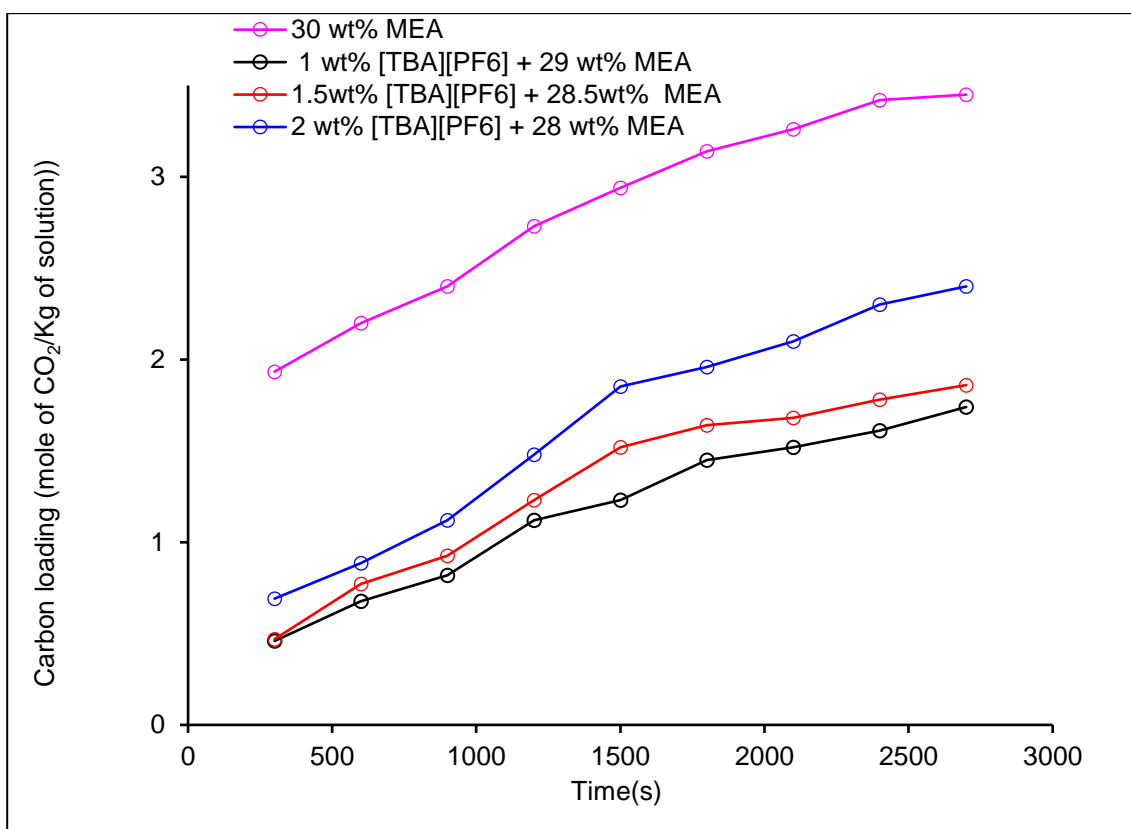


**Figure 6b.** Time and concentration dependence of carbon loading of non-aqueous MEA-[TBA][PF<sub>6</sub>] after absorption

#### 4. CONCLUSION

The thermophysical characteristics study of non-aqueous solvent mix of monoethanolamine (MEA) and tetrabutylammonium hexafluorophosphate [TBA][PF<sub>6</sub>] were determined experimentally at different concentrations and temperatures. Physical attributes were observed to rise with higher concentrations of [TBA][PF<sub>6</sub>] and decrease with higher temperatures as the kinetic energies of the molecules increase, which causes their intermolecular forces of attraction to weaken. Anion plays an important role in CO<sub>2</sub> absorption than cation of ILs. Carbon loading was higher at 2wt% IL+28wt% MEA when compared to other compositions, and this may need less regeneration energy than 30wt% MEA, despite the higher viscosity for this composition. The non-aqueous blend of MEA and [TBA][PF<sub>6</sub>] can be a good absorbent for CO<sub>2</sub> separation.

355 **Acknowledgment**

356 The authors gratefully acknowledge funding from the SCIENCE & ENGINEERING RESEARCH  
357 BOARD (SERB) - FILE NO. ECR/2016/001744 (a statutory body of the Department of Science &  
358 Technology, Government of India) New Delhi, India. The lab facility and research inspiration provided  
359 by SSN Trust, Sri Sivasubramaniya Nadar College of Engineering, Chennai, India, are sincerely  
360 acknowledged.

361 **References**

362 Aghel B., Janati S., Wongwises S., Shadloo M.S. (2022). Review on CO<sub>2</sub> capture by blended amine  
363 solutions, *International Journal of Greenhouse Gas Control*, **119**, 103715.  
364 <https://doi.org/10.1016/j.ijggc.2022.103715>.

365 Amirkhani F., Dashti A., Jokar M., Mohammadi A.H., Chofreh, A.G., Varbanov, P.S. and Zhou, J.L.  
366 (2023). Estimation of CO<sub>2</sub> solubility in aqueous solutions of commonly used blended amines:  
367 Application to optimised greenhouse gas capture. *Journal of Cleaner Production*, **430**, 139435.  
368 <https://doi.org/10.1016/j.chemosphere.2024.142792>.

369 Kontos G., Leontiadis K. and Tsivintzelis I. (2023). CO<sub>2</sub> solubility in aqueous solutions of blended  
370 amines: Experimental data for mixtures with MDEA, AMP and MPA and modeling with the modified  
371 Kent-Eisenberg model. *Fluid Phase Equilibria*, **570**, 113800.  
372 <https://doi.org/10.1016/j.fluid.2023.113800>.

373 Elmobarak W.F., Almomani F., Tawalbeh M., Al-Othman A., Martis R., Rasool K. (2023). Current status  
374 of CO<sub>2</sub> capture with ionic liquids: Development and progress, *Fuel*, **344**, 128102.  
375 <https://doi.org/10.1016/j.fuel.2023.128102>.

376 Shojaeian A., Hanifehei M., Fatoorehchi H. (2021). Density, Viscosity, and Refractive Index  
377 Measurements for Binary Mixtures of N-Methyldiethanolamine (MDEA), Diethanolamine (DEA), and  
378 2-Amino-2-methyl-1-propanol (AMP) with 1-Ethyl-3-methylimidazolium Acetate ([Emim][Ac]),  
379 *Journal of Chemical & Engineering Data*, **66(9)**, 3520-3530. <https://doi.org/10.1021/acs.jced.1c00387>.

380 Yan T., Chang X.L. and Pan W.G. (2024). Task-specific ionic liquids for carbon dioxide conversion into  
381 valuable chemical products: A review. *Journal of Industrial and Engineering Chemistry*.  
382 <https://doi.org/10.1016/j.jiec.2024.01.064>.

383 Orhan O.Y. (2021). Effects of various anions and cations in ionic liquids on CO<sub>2</sub> capture. *Journal of*  
384 *Molecular Liquids*, **333**, 115981. <https://doi.org/10.1016/j.molliq.2021.115981>.

385 Noorani N., Mehrdad A. and Ahadzadeh I. (2021). CO<sub>2</sub> absorption in amino acid-based ionic liquids:  
386 Experimental and theoretical studies. *Fluid Phase Equilibria*, **547**, 113185.  
387 <https://doi.org/10.1016/j.fluid.2021.113185>.

388 Perumal M., Balraj A., Jayaraman D., Krishnan J., (2020). Experimental investigation of density,  
389 viscosity, and surface tension of aqueous tetrabutylammonium-based ionic liquids, *Environmental*  
390 *Science and Pollution Research*, **28**, 63599-63613. <https://doi.org/10.1007/s11356-020-11174-4>.

391 Kartikawati N.A., Safdar R., Lal B., Mutalib MIBA, Shariff A.M. (2018). Measurement and correlation  
392 of the physical properties of aqueous solutions of ammonium based ionic liquids, *Journal of Molecular*  
393 *Liquids*, **253**, 250-258. <https://doi.org/10.1016/j.molliq.2018.01.040>.

394 Yusoff R., Shamiri A., Aroua M.K., Ahmady A., Shafeeyan M.S., Lee W.S., Lim S.L. and Burhanuddin  
395 S.N.M. (2014). Physical properties of aqueous mixtures of N-methyldiethanolamine (MDEA) and ionic  
396 liquids, *Journal of Industrial and Engineering Chemistry*, **20(5)**, 3349-3355.  
397 <https://doi.org/10.1016/j.jiec.2013.12.019>.



398 Perumal M., Jayaraman D. and Balraj A. (2021). Experimental studies on CO<sub>2</sub> absorption and solvent  
399 recovery in aqueous blends of monoethanolamine and tetrabutylammonium hydroxide. *Chemosphere*,  
400 **276**, 130159. <https://doi.org/10.1016/j.chemosphere.2021.130159>.

401 Khan S.N., Hailegiorgis S.M., Man Z., Shariff A.M., Garg S. (2017). Thermophysical properties of  
402 concentrated aqueous solution of N-methyldiethanolamine (MDEA), piperazine (PZ), and ionic liquids  
403 hybrid solvent for CO<sub>2</sub> capture, *Journal of Molecular Liquids*, **229**, 221-229.  
404 <https://doi.org/10.1016/j.molliq.2016.12.056>.

405 Ab Rahim A. H., Yunus N. M., Jaffar Z., Allim M. F., Zailani N. Z. O., Fariddudin S. A. M., ... & Umar  
406 M. (2023). Synthesis and characterization of ammonium-based protic ionic liquids for carbon dioxide  
407 absorption, *RSC advances*, **13(21)**, 14268-14280.

408 Wu Y., Xu J., Mumford K., Stevens G.W., Fei W., Wang Y. (2020). Recent advances in carbon dioxide  
409 capture and utilization with amines and ionic liquids, *Green Chemical Engineering*, **1(1)**, 16-32.  
410 <https://doi.org/10.1016/j.gce.2020.09.005>.

411 Baj S., Siewniak A., Chrobok A., Krawczyk T., Sobolewski A. (2013). Monoethanolamine and ionic  
412 liquid aqueous solutions as effective systems for CO<sub>2</sub> capture, *Journal of Chemical Technology &*  
413 *Biotechnology*, **88(7)**, 1220-1227. <https://doi.org/10.1002/jctb.3958>.

414 Mazari S.A., Siyal A.R., Solangi N.H., Ahmed S., Griffin G., Abro R., Mubarak N.M., Ahmed M. and  
415 Sabzoi N. (2021). Prediction of thermo-physical properties of 1-Butyl-3-methylimidazolium  
416 hexafluorophosphate for CO<sub>2</sub> capture using machine learning models. *Journal of Molecular*  
417 *Liquids*, **327**, 114785. <https://doi.org/10.1016/j.molliq.2020.114785>.

418 Halim N.H., Yunus N.M. (2018, September). Thermophysical properties and CO<sub>2</sub> absorption of  
419 ammonium-based ionic liquids. In AIP Conference Proceedings, AIP Publishing, **2016(1)**.  
420 <https://doi.org/10.3390/pr7110820>.

421 Yunus N.M., Halim N.H., Wilfred C.D., Murugesan T., Lim J.W., Show P.L. (2019). Thermophysical  
422 properties and CO<sub>2</sub> absorption of ammonium-based protic ionic liquids containing acetate and butyrate  
423 anions, *Processes*, **7(11)**, 820. <https://doi.org/10.3390/pr7110820>.

424 Wang C., Xie Y., Li W., Ren Q., Lv B., Jing G., & Zhou Z. (2023). Performance and mechanism of the  
425 functional ionic liquid absorbent with the self-extraction property for CO<sub>2</sub> capture, *Chemical*  
426 *Engineering Journal*, **473**, 145266. <https://doi.org/10.1016/j.cej.2023.145266>.

427 Ramkumar V. and Gardas R.L. (2019). Thermophysical properties and carbon dioxide absorption studies  
428 of guanidinium-based carboxylate ionic liquids. *Journal of Chemical & Engineering Data*, **64(11)**, 4844-  
429 4855. <https://doi.org/10.1021/acs.jced.9b00377>.

430 Wei L., Guo R., Tang Y., Zhu J., Liu M., Chen J., et al. (2020). Properties of aqueous amine based protic  
431 ionic liquids and its application for CO<sub>2</sub> quick capture, *Separation and Purification Technology*, **239**,  
432 116531. <https://doi.org/10.3390/molecules27030851>.

433 Li C., Zhao T., Yang A., & Liu F. (2021). Highly efficient absorption of CO<sub>2</sub> by protic ionic liquids-  
434 amine blends at high temperatures, *ACS omega*, **6(49)**, 34027-34034.

435 Hafizi A., Rajabzadeh M., Mokari M.H., Khalifeh R. (2021). Synthesis, property analysis and absorption  
436 efficiency of newly prepared tricationic ionic liquids for CO<sub>2</sub> capture, *Journal of Molecular Liquids*, **324**,  
437 115108. <https://doi.org/10.1016/j.molliq.2020.115108>.

438 Zhang X., Zhang X., Dong H., Zhao Z., Zhang S., Huang Y. (2012). Carbon capture with ionic liquids:  
439 overview and progress, *Energy & Environmental Science*, **5(5)**, 6668-6681.  
440 <https://doi.org/10.1039/C2ee21152a>.

441 Boualem A.D., Argoub K., Benkouider A.M., Yahiaoui A. and Toubal K. (2022). Viscosity prediction  
442 of ionic liquids using NLR and SVM approaches. *Journal of Molecular Liquids*, **368**, 120610.  
443 <https://doi.org/10.1016/j.molliq.2022.120610>.

444 Latini G., Signorile M., Rosso F., Fin A., d'Amora M., Giordani S. (2022). Efficient and reversible CO<sub>2</sub>  
445 capture in bio-based ionic liquids solutions, *Journal of CO<sub>2</sub> Utilization*, **55**, 101815.  
446 <https://doi.org/10.1016/j.jcou.2021.101815>.

447 Theo W.L., Lim J.S., Hashim H., Mustaffa A.A., Ho W.S. (2016). Review of pre-combustion capture  
448 and ionic liquid in carbon capture and storage, *Applied energy*, **183**, 1633-1663.  
449 <https://doi.org/10.1016/j.apenergy.2016.09.103>.

450 Perumal M., & Jayaraman D. (2023). Amine-Ionic Liquid Blends in CO<sub>2</sub> Capture Process for  
451 Sustainable Energy and Environment, *Energy & Environment*, **34(3)**, 517-532.  
452 <https://doi.org/10.1177/0958305X211070782>.

453 Hasib-ur-Rahman M., Siaj M., Larachi F. (2010). Ionic liquids for CO<sub>2</sub> capture-Development and  
454 progress, *Chemical Engineering and Processing: Process Intensification*, **49(4)**, 313-322.  
455 <https://doi.org/10.1016/j.cep.2010.03.008>.

456 Amirchand K. D., & Singh V. (2022). Density, speed of sound, and surface tension of binary aqueous  
457 solutions containing ammonium based protic ionic liquids, *Journal of Molecular Liquids*, **354**, 118845.  
458 <https://doi.org/10.1016/j.molliq.2022.118845>.

459 Zacchello B., Oko E., Wang M., Fethi A. (2017). Process simulation and analysis of carbon capture with  
460 an aqueous mixture of ionic liquid and monoethanolamine solvent, *International Journal of Coal Science  
& Technology*, **4**, 25-32. <https://doi.org/10.1007/s40789-016-0150-1>.

462 Torralba-Calleja E., Skinner J., Gutiérrez-Tauste D. (2013). CO<sub>2</sub> capture in ionic liquids: A review of  
463 solubilities and experimental methods, *Journal of Chemistry*, **2013**, 1-16.  
464 <https://doi.org/10.1155/2013/473584>.

465 Numpilai T., Pham L.K.H. and Witoon T. (2024). Advances in Ionic Liquid Technologies for CO<sub>2</sub>  
466 Capture and Conversion: A Comprehensive Review. *Industrial & Engineering Chemistry Research*.

467 Choi B. K., Kim S. M., Kim K. M., Lee U., Choi J. H., Lee J. S., ... & Moon J. H. (2021). Amine  
468 blending optimization for maximizing CO<sub>2</sub> absorption capacity in a diisopropanolamine–  
469 methyldiethanolamine–H<sub>2</sub>O system using the electrolyte UNIQUAC model, *Chemical Engineering*  
470 *Journal*, **419**, 129517. <https://doi.org/10.1016/j.cej.2021.129517>.

471 Shukla S.K., Khokarale S.G., Bui T.Q., Mikkola J.P.T. (2019). Ionic liquids: Potential materials for  
472 carbon dioxide capture and utilization, *Frontiers in Materials*, **6**, 42.  
473 <https://doi.org/10.3389/fmats.2019.00042>.

474 Kaviani S., Kolahchyan S., Hickenbottom K.L., Lopez A.M., Nejati S. (2018). Enhanced solubility of  
475 carbon dioxide for encapsulated ionic liquids in polymeric materials, *Chemical Engineering Journal*,  
476 **354**, 753-757. <https://doi.org/10.1016/j.cej.2018.08.086>.

477 Ma Y., Gao J., Wang Y., Hu J., Cui P. (2018). Ionic liquid-based CO<sub>2</sub> capture in power plants for low  
478 carbon emissions, *International Journal of Greenhouse Gas Control*, **75**, 134-139.  
479 <https://doi.org/10.1016/j.ijggc.2018.05.025>.

480 Yang X., Zhu C., Fu T. and Ma Y. (2024). A novel synergistic intensification method for CO<sub>2</sub> absorption  
481 by metal salt and task-specific ionic liquids hybrid solvent in microchannel reactor. *International Journal*  
482 *of Heat and Mass Transfer*, **222**, 125210. <https://doi.org/10.1016/j.ijheatmasstransfer.2024.125210>.

- 483 Brennecke J.F., Gurkan B.E. (2010). Ionic liquids for CO<sub>2</sub> capture and emission reduction, *The Journal*  
484 *of Physical Chemistry Letters*, **1(24)**, 3459-3464. <https://doi.org/10.1021/jz1014828>.
- 485 Abraham M.H., Acree Jr W.E., Hoekman D., Leo A.J. and Medlin M.L. (2019). A new method for the  
486 determination of Henry's law constants (air-water-partition coefficients). *Fluid Phase Equilibria*, **502**,  
487 112300. <https://doi.org/10.1016/j.fluid.2019.112300>.
- 488 Shohrat A., Zhang M., Hu H., Yang X., Liu L. and Huang, H. (2022). Mechanism study on CO<sub>2</sub> capture  
489 by ionic liquids made from TFA blended with MEA and MDEA. *International Journal of Greenhouse*  
490 *Gas Control*, **119**, 103709. <https://doi.org/10.1016/j.ijggc.2022.103709>.
- 491 Yang L., Chen J., Ma N., Li X., & Huang Z. (2023). CO<sub>2</sub> absorption enhancement of fluorinated ionic  
492 liquids on nonaqueous biphasic absorbents: Experimental and theoretical study, *Carbon Capture*  
493 *Science & Technology*, **9**, 100147. <https://doi.org/10.1016/j.ccst.2023.100147>.